# Displacement Distribution of a freely Oscillating Rutile Sphere

Tôhoku Geophys. Journ. (Sci. Rep. Tôhoku Univ., Ser. 5), Vol. 32, Nos. 3, 4, pp. 55-76, 1990 

# *Displacement Distribution of a Freely Oscillating Rutile Sphere*

SATORU ISODA[1], HITOSHI ODA, ISAO SUZUKI, and KIYOSHI SEYA

Department of Earth Sciences, Faculty of Science
Okayama University, Okayama 700

(Received November 16, 1989)

*Abstract*: In order to clarify free oscillations of an elastically anisotropic sphere, the eigenfrequencies and displacements were computed by the Rayleigh-Ritz method for a single crystal rutile sphere. The oscillation modes of the sphere are classified into ten groups belonging to the point group $D_{4h}$. The present method of numerical computation can also be applied to crystals with other symmetries, and may be useful to study anisotropic Earth's free oscillation as well as to determine elastic constants of small specimens by laboratory measurements.

We confirm that the computed eigenfrequencies satisfactorily agree with the observed ones and that all the computed displacement distributions satisfy the symmetric properties required by the group theory on the point group $D_{4h}$. The displacement patterns in some fundamental modes are similar to those of an isotropic sphere. However, they significantly differ from those of the isotropic cases in other fundamental modes as well as in all the higher modes. The displacement distributions are remarkably affected by the anisotropic elasticity as a result of extensive coupling among toroidal (torsional) and spheroidal modes of a reference isotropic sphere, and the strength of the coupling varies from mode to mode. Two different displacement distributions are obtained for a two-fold degenerate mode, and they are geometrically the same.

## 1. Introduction

The analytic solutions of free vibration of a homogeneous "isotropic" sphere were derived by Lamb (1882) for toroidal (torsional) and spheroidal modes. Applying the theory, Sato and Usami (1962) computed eigenfrequencies of a vibrating sphere and depicted the displacement distribution in it. These works founded a base in the studies of free oscillation of the Earth and, further, of its structure (*e.g.*, Jordan and Anderson, 1974). On the other hand, the theory was also applied to determination of elastic constants of isotropic materials by comparing the computed eigenfrequencies with the observed ones of sphere specimens (*e.g.*, Soga and Anderson, 1967).

Modern seismology has revealed that the earth has "anisotropic" properties, especially in the upper mantle and in the inner core (Suetsugu and Nakanishi, 1987; Morelli *et al.*, 1986; Woodhouse *et al.*, 1986). Therefore, necessity has increased to study the free oscillations of spheres with anisotropic elasticity. However, differing from isotropic spheres, no practical method was available to compute eigenfrequencies of

[1] Now at the Matsushita Soft Research Co. in Osaka

anisotropic ones. If such computation becomes possible, it must be useful not only for laboratory measurements of elastic constants of anisotropic solids but also for studies of the anisotropic properties of the Earth.

It was quite recent that Mochizuki (1988) developed the theory of free oscillations of homogeneous spheres with general elastic anisotropy and that Oda *et al.* (1988) developed computer algorithm and programs to evaluate their eigenfrequencies by the Rayleigh-Ritz method. Through these basic studies, the resonant sphere technique (RST) has become applicable for accurate determination of elastic constants of single crystals such as rutile ($TiO_2$) and periclase (MgO) (Suzuki *et al.*, 1988 ; Oda *et al.*, 1989). However, it is not clarified yet how an elastically anisotropic sphere vibrates, since the displacement field due to the free oscillation is not analytically expressed.

In this paper, we show the results of computation to obtain free oscillation eigenfrequencies and displacements of a rutile sphere, whose crystal symmetry is tetragonal. The computed eigenfrequencies are compared with the observed ones. The displacement patterns of the vibrating rutile sphere are compared with those of an isotropic one to clarify the effects of anisotropic elasticity. The symmetry of the displacement patterns is investigated based on the group theory. Through these examinations, we will clarify the characteristics of the free oscillation of a sphere with the tetragonal symmetry and confirm that the present computer algorithm and programs are correctly composed and useful for future applications.

## 2. Compuation Method

In this section, we briefly review the basic part of the Mochizuki's theory (Mochizuki, 1988) for the present computation of free oscillation eigenfrequencies and displacememts. For this purpose, we introduce the spherical coordinate system ($\theta$, $\phi$, $r$), whose origin is the center of the sphere under consideration (Phinney and Burridge, 1973). The free oscillation of a sphere can be described by applying the variational principle to an energy equation,

$$\delta \int (\rho\omega^2 U_i^* U_i - \varepsilon_{ij}^* K_{ijkl} \varepsilon_{kl}) dV = 0 \tag{1}$$

where the first and second terms denote kinetic and strain energies, respectively, and the integration is made over the entire sphere. The $\rho$ is density and the $\omega$ is angular eigenfrequency ($=2\pi f$). The $\boldsymbol{U}$ is displacement vector, the $\varepsilon$ is strain tensor, and the $\boldsymbol{K}$ is elastic constant tensor, all defined by the spherical coordinates. The indices $i$, $j$, $k$, and $l$ are understood to take one of ($\theta$, $\phi$, $r$), and the summation convention is assumed for the repeated indices. The asterisk denotes the complex conjugate. The $\boldsymbol{K}$ is related to the elastic constant tensor $\boldsymbol{C}$ defined by the Cartesian coordinate system ($x$, $y$, $z$) as

$$K_{ijkl} = T_{ii'} T_{jj'} T_{kk'} T_{ll'} C_{i'j'k'l'} \tag{2}$$

where the $i'$, $j'$, $k'$ and $l'$ take one of ($x$, $y$, $z$) or the corresponding indices (1, 2, 3), and the conversion matrix $\boldsymbol{T}$ is defined by

$$\boldsymbol{T}=(T_{ii'})=\begin{pmatrix}\cos\theta\cos\phi & \cos\theta\sin\phi & -\sin\theta\\ -\sin\phi & \cos\phi & 0\\ \sin\theta\cos\phi & \sin\theta\sin\phi & \cos\theta\end{pmatrix} \tag{3}$$

In applying the Rayleigh-Ritz method, the displacement vector $\boldsymbol{U}$ is expressed by a linear combination of known normalized orthogonal basis function vectors $\boldsymbol{v}^p$ as

$$\boldsymbol{U}=\sum_p a_p\boldsymbol{v}^p \tag{4}$$

where the $a_p(p=1, 2, \ldots)$ are unknown coefficients to be determined as shown below. Substituting (4) into (1), we obtain a set of linear equations,

$$\sum_q(\omega^2\langle p\mid\rho\mid q\rangle-\langle p\mid\boldsymbol{K}\mid q\rangle)a_q=0,\ (p=1, 2, \ldots) \tag{5}$$

These are eigenvalue equations, and the $\omega^2$ and $a_p$ $(p=1, 2, \ldots)$ are the eigenvalue and eigenvector, respectively. The matrix elements $\langle p\mid\rho\mid q\rangle$ and $\langle p\mid\boldsymbol{K}\mid q\rangle$ are expressed as

$$\begin{aligned}\langle p\mid\rho\mid q\rangle&=\int v_i^{p*}\rho v_i^q dV\\ \langle p\mid\boldsymbol{K}\mid q\rangle&=\int\varepsilon_{ij}^{p*}K_{ijkl}\varepsilon_{kl}^q dV\end{aligned} \tag{6}$$

and the $\boldsymbol{\varepsilon}^p$ are the strain tensor from the $\boldsymbol{v}^p$. The $\langle p\mid\rho\mid q\rangle$ and $\langle p\mid\boldsymbol{K}\mid q\rangle$ are Hermitian matrices, and all the eigenvalues in (5) are real. Solving the eigenvalue equations for a given elastic constant tensor $\boldsymbol{C}$ under the normalization condition

$$\sum_p a_p a_p^*=1, \tag{7}$$

we can simultaneously obtain both of the eigenvalues and the eigenvectors. The free oscillation displacement is found by substituting the eigenvector $a_p$ into (4).

It may be natural to adopt the normalized free oscillation eigenfunctions of a homogeneous isotropic sphere as the basis functions. For tetragonal elastic anisotropy, the basis functions are expressed as

$$\boldsymbol{v}^p=\mid p\rangle=\mid Onlmh\rangle \tag{8}$$

where the parameter $p$ denotes a set of parameters $(O, n, l, m, h)$. The $O$ means toroidal (T) or spheroidal (S) oscillation mode, the $n$, $l$ and $m$ are radial, angular and azimuthal orders, respectively, and the $h$ takes $c$ or $s$ as defined in (9). Then, the basis functions are written as

$$\begin{aligned}\mid Onlmc\rangle&=[\mid Onlm\rangle+(-1)^m\mid Onl-m\rangle]/2\ ;\ l\geqq m\geqq 0\\ \mid Onlms\rangle&=[\mid Onlm\rangle-(-1)^m\mid Onl-m\rangle]/2i\ ;\ l\geqq m\geqq 1\end{aligned} \tag{9}$$

where the $i$ denotes $(-1)^{1/2}$.

When the basis functions are orthogonally normalized and the density is assumed to be uniform over the entire sphere, the kinetic energy matrix $\langle p\mid\rho\mid q\rangle$ in (6) has non-zero values only in the diagonal elements, *i.e.*,

$$\langle p\mid\rho\mid q\rangle=\rho\delta_{pq} \tag{10}$$

Table 1. Grouping of the Basis Functions for the Rutile Sphere and the Number $N_b$ of the Basis Functions Used in the Present Computation

| Group | Basis Function | | $N_b$ |
|---|---|---|---|
| $A_{1g}$ : | ${}_nS_{2l}^{4mc}$, ${}_nT_{2l'+1}^{4m's}$ | | 78 |
| $B_{1g}$ : | ${}_nS_{2l}^{4m+2c}$, ${}_nT_{2l'+1}^{4m'+2s}$ | | 72 |
| $A_{2g}$ : | ${}_nS_{2l}^{4ms}$, ${}_nT_{2l'+1}^{4m'c}$ | | 77 |
| $B_{2g}$ : | ${}_nS_{2l}^{4m+2s}$, ${}_nT_{2l'+1}^{4m'+2c}$ | | 72 |
| $E_g$ : | ${}_nS_{2l}^{2m+1c}$, ${}_nT_{2l'+1}^{2m'+1s}$ | degenerate | 149 |
| | ${}_nS_{2l}^{2m+1s}$, ${}_nT_{2l'+1}^{2m'+1c}$ | | 149 |
| $A_{1u}$ : | ${}_nS_{2l+1}^{4ms}$, ${}_nT_{2l'}^{4m'c}$ | | 72 |
| $B_{1u}$ : | ${}_nS_{2l+1}^{4m+2s}$, ${}_nT_{2l'}^{4m'+2c}$ | | 72 |
| $A_{2u}$ : | ${}_nS_{2l+1}^{4mc}$, ${}_nT_{2l'}^{4m's}$ | | 77 |
| $B_{2u}$ : | ${}_nS_{2l+1}^{4m+2c}$, ${}_nT_{2l'}^{4m'+2s}$ | | 72 |
| $E_u$ : | ${}_nS_{2l+1}^{2m+1c}$, ${}_nT_{2l'}^{2m'+1s}$ | degenerate | 149 |
| | ${}_nS_{2l+1}^{2m+1s}$, ${}_nT_{2l'}^{2m'+1c}$ | | 149 |

The ${}_nO_l^{mh}$ denotes $|\, Onlmh\rangle$. The $A_{1g}$, $B_{1g}$, ... and $E_u$ are irreducible representations of the point group $D_{4h}$. The oscillation modes in $E_g$ and $E_u$ groups are two-fold degenerate. (after Mochizuki, 1988)

where $\delta_{pq}$ is the Kronecker's delta; $\delta_{pq}=1$ for $p=q$ and $\delta_{pq}=0$ for $p\neq q$. Recently, Mochizuki (1986, 1988) presented an explicit expression for the matrix elements $\langle p \mid \boldsymbol{K} \mid q\rangle$ of the strain energy. He classified the basis functions into several groups, based on the characteristics of the matrix element $\langle p \mid \boldsymbol{K} \mid q\rangle$ governed by the crystal symmetry. Then, the strain energy matrix can be block-diagonalized with smaller submatrices, each of which consists of the basis functions belonging to one of the groups. Evaluation of the elements $\langle p \mid \boldsymbol{K} \mid q\rangle$ become possible through recent efforts by the present authors. The eigenfrequencies and eigenvectors are obtained by solving the eigenvalue equations (5), and hence, the vibrational displacements by (4). The oscillation patterns in each group must satisfy the common symmetric properties to the group as shown later (*cf.*, Table 4).

The basis functions used in the present computation are classified into ten groups as shown in Table 1, where $A_{1g}$, $B_{1g}$, ..., $E_u$ are irreducible representations of the point group $D_{4h}$. The basis functions both for $E_g$ and $E_u$ groups are further divided into two groups, from which the same eigenfrequencies are obtained. In this meaning, the $E_g$ and $E_u$ groups are called two-fold degenerate modes.

## 3. Results

We observed the oscillatory spectra of a single crystal rutile sphere with the diameter and density listed in Table 2. An example of the spectra is shown in Fig. 1. The eigenfrequencies of the isotropic modes, S and T, of a sphere with the same diameter and the isotropic elastic constants given by the Hill averages (Kumazawa, 1964), are calculated and also shown in Fig. 1 for comparison. It is apparent that every tetragonal

Table 2. Physical Parameters of the Rutile Sphere

| Diameter = 8.194 mm | | |
|---|---|---|
| Density = 4.2539 g/cm³ | | |
| Elastic Constants in GPa | | |
| $ij$ | ${}^{w}C_{ij}$ | ${}^{1}C_{ij}$ |
| 11 | 266.0 | 267.0 |
| 33 | 469.9 | 485.3 |
| 44 | 123.9 | 123.3 |
| 66 | 188.6 | 191.7 |
| 12 | 173.4 | 176.4 |
| 13 | 136.2 | 149.6 |
| Isotropic Elastic Constants in GPa | | |
| $K_S$ | 206.7 | 213.9 |
| $\mu$ | 111.8 | 110.7 |
| $\nu$ | 0.2709 | 0.2793 † |

${}^{w}C$: Wachtman *et al.*, (1962). Used as the reference values
${}^{1}C$: the present specimen determined by the least squares calculation
$K_S$: bulk modulus, $\mu$: rigidity, and $\nu$: Poisson's ratio. All are the Voigt-Reuss-Hill averages (Kumazawa, 1964).
†: dimensionless

mode comes from splittings of the isotropic modes due to its lower symmetry. The only exception in the figure is the $A_{1g}-2$ mode which is a singlet and comes directly from the ${}_0S_0$ mode. Further, anisotropic splittings of degenerate modes complete in the orthorhombic symmetry lower than the tetragonal (Isoda, 1989). The absolute values of resonance frequencies $f^0$ were measured through a similar way to that in the RPR method (*e.g.*, Ohno, 1976), and are listed in Table 3. The lowest 43 modes beginning at 0.35 MHz are identified by comparing them with the computed eigenfrequencies.

Based on the data in Table 2, we computed the eigenfrequencies of the rutile sphere. For the basis functions $|\,Onlmh\rangle$ in the present computation, we used the eigenfunctions of an isotropic sphere with the Poisson's ratio of 0.25. Using the Poisson's ratio of 0.25 different from 0.2709 in Table 2 does not seriously affect the results in the present work (*cf.*, Isoda, 1989). The eigenfunctions are totally 1188 singlets from 59 spheroidal multiplets (${}_0S_0$, ${}_0S_2-{}_0S_9$, ${}_1S_0-{}_1S_9$, ${}_2S_0-{}_2S_9$, ${}_3S_0-{}_3S_9$, ${}_4S_0-{}_4S_9$ and ${}_5S_0-{}_5S_9$) and 53 toroidal multiplets (${}_0T_2-{}_0T_9$, ${}_1T_1-{}_1T_9$, ${}_2T_1-{}_2T_9$, ${}_3T_1-{}_3T_9$, ${}_4T_1-{}_4T_9$ and ${}_5T_1-{}_5T_9$), and each multiplet is specified by its dimensionless isotropic eigenvalue $\eta$ or the orders $n$ and $l$. The number of the basis functions used for each group is shown in Table 1. Although we need only some tens of the eigenfrequencies of the specimen, such a large number of basis functions are necessary to obtain sufficiently accurate eigenfrequencies

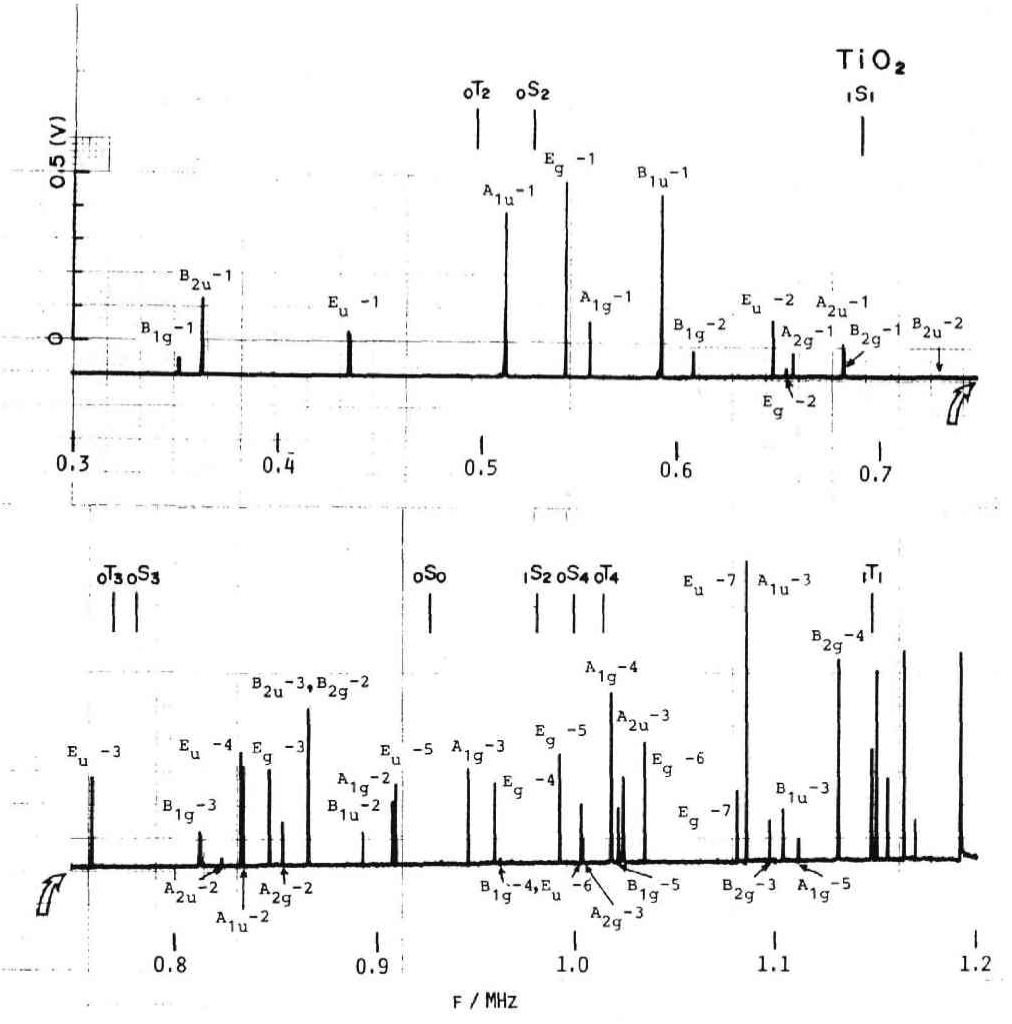


Fig. 1 An observed free oscillation spectrum of the rutile ($TiO_2$) sphere. The lower 43 modes are designated through the irreducible group name. Their amplitudes are changed when the specimen is rotated relatively to the transducers. The Hill averages of elastic constants (Table 2) give isotropic frequencies designated by ${}_nS_l$ (spheroidal) and ${}_nT_l$ (torsional).

and eigenvectors $a_p$ from (5). Each anisotropic mode specified by its eigenfrequency is designated by its irreducible group name and by the sequential number counted from the fundamental mode to a higher mode in the group. The lowest 43 eigenfrequencies $f^w$ computed are listed in Table 3, and compared with the observed eigenfrequencies $f^0$. The differences between $f^0$ and $f^w$ are fairly small (Table 3). This suggests that the present computer algorithm and programs are correctly composed. The differences between $f^0$ and $f^w$ are due to small differences between the elastic constants of the present specimen and the values adopted in computation, ${}^wC_{ij}$ in Table 2. By using these

Table 3. Comparison of the Computed and Observed Eigenfrequencies of the Rutile Sphere[1)]

| No. | Mode | $f^w$/kHz | $f^1$/kHz | $f^0$/kHz | $\Delta$ |
|---|---|---|---|---|---|
| 1 | $B_{1g}$ -1 | 351.06 | 347.58 | 351.12 | 1.01 |
| 2 | $B_{2u}$ -1 | 365.33 | 361.88 | 361.86 | 0.00 |
| 3 | $E_u$ -1 | 439.66 | 435.22 | 434.01 | −0.28 |
| 4 | $A_{1u}$ -1 | 512.86 | 511.26 | 511.27 | 0.00 |
| 5 | $E_g$ -1 | 542.08 | 540.28 | 540.86 | 0.11 |
| 6 | $A_{1g}$ -1 | 559.54 | 550.72 | 552.89 | 0.39 |
| 7 | $B_{1u}$ -1 | 586.64 | 588.20 | 587.99 | −0.04 |
| 8 | $B_{1g}$ -2 | 620.91 | 614.03 | 608.94 | −0.84 |
| 9 | $E_u$ -2 | 648.59 | 645.58 | 647.71 | 0.33 |
| 10 | $E_g$ -2 | 658.33 | 654.55 | 654.50 | −0.01 |
| 11 | $A_{2g}$ -1 | 659.57 | 653.84 | 657.56 | 0.57 |
| 12 | $A_{2u}$ -1 | 685.70 | 680.28 | 681.65 | 0.20 |
| 13 | $B_{2g}$ -1 | 673.76 | 680.70 | 682.39 | 0.25 |
| 14 | $B_{2u}$ -2 | 733.83 | 730.86 | 730.95 | 0.01 |
| 15 | $E_u$ -3 | 765.17 | 761.84 | 759.32 | −0.33 |
| 16 | $B_{1g}$ -3 | 816.39 | 814.88 | 811.64 | −0.40 |
| 17 | $A_{2u}$ -2 | 826.66 | 820.67 | 822.99 | 0.28 |
| 18 | $E_u$ -4 | 838.42 | 830.81 | 831.87 | 0.13 |
| 19 | $A_{1u}$ -2 | 838.00 | 832.11 | 833.35 | 0.15 |
| 20 | $E_g$ -3 | 850.30 | 847.99 | 846.26 | −0.20 |
| 21 | $A_{2g}$ -2 | 855.57 | 853.20 | 852.79 | −0.05 |
| 22 | $B_{2u}$ -3 | 870.74 | 865.27 | 865.70 | 0.05 |
| 23 | $B_{2g}$ -2 | 873.45 | 867.29 | 866.14 | −0.13 |
| 24 | $B_{1u}$ -2 | 888.04 | 891.94 | 893.04 | 0.12 |
| 25 | $A_{1g}$ -2 | 904.10 | 905.53 | 908.51 | 0.33 |
| 26 | $E_u$ -5 | 904.10 | 910.19 | 910.04 | −0.02 |
| 27 | $A_{1g}$ -3 | 941.17 | 946.27 | 946.16 | −0.01 |
| 28 | $E_g$ -4 | 965.96 | 958.69 | 959.48 | 0.08 |
| 29 | $B_{1g}$ -4 | 972.59 | 964.09 | 962.08 | −0.21 |
| 30 | $E_g$ -5 | 992.81 | 992.03 | 991.83 | −0.02 |
| 31 | $E_u$ -6 | 1008.70 | 1004.75 | 1003.75 | −0.10 |
| 32 | $A_{2g}$ -3 | 1016.45 | 1007.77 | 1004.53 | −0.32 |
| 33 | $A_{1g}$ -4 | 1023.49 | 1019.53 | 1018.85 | −0.07 |
| 34 | $B_{1g}$ -5 | 1030.28 | 1022.02 | 1022.44 | 0.04 |
| 35 | $A_{2u}$ -3 | 1026.15 | 1023.62 | 1024.68 | 0.10 |
| 36 | $E_g$ -6 | 1041.35 | 1035.04 | 1035.57 | 0.05 |
| 37 | $E_g$ -7 | 1081.10 | 1079.46 | 1081.29 | 0.17 |
| 38 | $E_u$ -7 | 1098.22 | 1092.85 | 1085.83 | −0.65 |
| 39 | $A_{1u}$ -3 | 1094.10 | 1090.48 | 1086.03 | −0.41 |
| 40 | $B_{2g}$ -3 | 1093.57 | 1098.82 | 1097.60 | −0.11 |
| 41 | $B_{1u}$ -3 | 1113.06 | 1105.24 | 1104.23 | −0.09 |
| 42 | $A_{1g}$ -5 | 1110.23 | 1112.08 | 1111.57 | −0.05 |
| 43 | $B_{2g}$ -4 | 1128.90 | 1133.55 | 1130.91 | −0.23 |

$f^w$ : computed eigenfrequencies based on the ${}^wC_{ij}$

$f^1$ : computed ones based on the ${}^1C_{ij}$ from the least squares calculation ; in both computation, $n_{max}=5$ and $l_{max}=9$.

$f^0$ : observed ones of the rutile sphere.

$\Delta$ : $100\times(f^0-f^1)/f^1$, in percent

1) After Suzuki *et al.*, (1988)

frequency differences, we can determine the specimen's elastic constants ${}^1C_{ij}$ as shown in Table 1. More details in determination will appear elsewhere (Suzuki *et al.*, in preparation).

Obtaining eigenfrequencies and eigenvectors, we compute free oscillation displacements by (4). Figures 2-a to 2-l show the displacement distributions of the fundamental modes in all the irreducible groups. The displacements are shown in the three sections of the $x$-$y$, $y$-$z$ and $z$-$x$ planes, where the $x$-, $y$- and $z$-axes are the $a$-, $b$- and $c$-axes of the tetragonal crystal, respectively. In each section, the compuation was made at ten points in 24 directions from the center to the surface. Because of the symmetric properties of the crystal or selected basis functions, the displacement vectors have no oblique component to the sections. The arrows in the figures thus show the displacement vectors laying on the section, and the crosses and the circles show those perpendicular to the section. The symbol size is proportional to the vibration amplitude at each point. These displacement patterns, however, cannot be compared with observed amplitude, since it is, at present, difficult to measure displacement experimentally even on the surface.

The distribution of displacement vectors varies from mode to mode. Most of the modes have no displacement at some points on the surface, called "nodal points". This may cause some difficulty in experimental observation of eigenfrequencies (*cf.*, see the $B_{2u}-2$ mode in Figure 1), if the sphere specimen could not be rotated to another orientation during measurement. Even though they are fundamental modes, the $A_{2u}-1$ and $E_u-1$ modes (Figs. 2-i, -k and -l) have significant magnitudes in displacement at and around the center of the sphere, owing to the contribution from the isotropic eigenfunction of the ${}_1S_1^n$ modes. This is one of the differences in free oscillations between isotropic and anisotropic spheres. It is noted in two-fold degenerate modes that the eigenfrequency gives two different distributions of displacements, $\boldsymbol{U}^1$ and $\boldsymbol{U}^2$. However, their displacement patterns are geometrically the same, because they are congruent with each other when either $\boldsymbol{U}^1$ or $\boldsymbol{U}^2$ is rotated by ninety degrees around the $z$-axis. Computations were made also in the (110) plane, as well as for higher modes in each group (Isoda, 1989), and the characteristics on the displacement distributions are also confirmed.

As understood from (4), the free oscillation displacement of anisotropic spheres is expressed by superposition of isotropic eigenfunctions (basis functions) weighted with expansion coefficients $a_p$. When only one of eigenfunctions mainly contributes to an anisotropic oscillation mode, the oscillation pattern is similar to that of the isotropic one, and otherwise it is different from that depending on degree of coupling with the other modes. Both the cases are found to take place in the oscillation of the rutile sphere.

Fig. 2 (a-l) Distributions of displacement vectors for the fundamental modes of ten groups. A cross means a vector directing upward perpendicular to the paper sheet, and an open circle is in the opposite direction. An arrow indicates the displacement vector on the plane. Symbol size is proportional to the magnitude of the displacement component. The plane indices (001), (100) and (010) denote the $x-y$, $y-z$ and $z-x$ planes, respectively. See text for the inserted $\eta-A$ diagram.

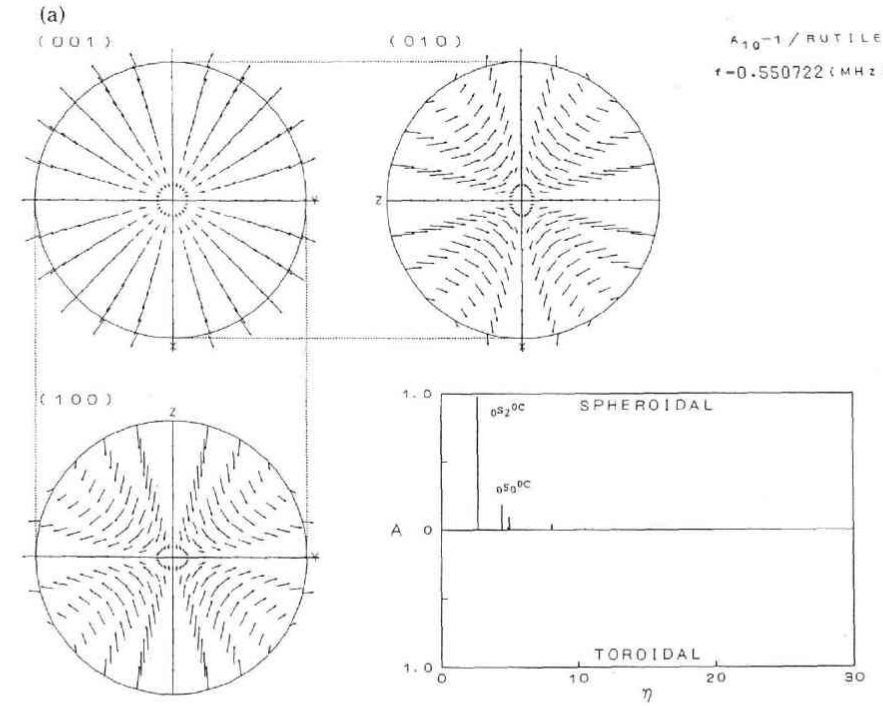
(a)
(001)
(010)
$A_{10}$-1 / RUTILE
f=0.550722 (MHz)
(100)
$_0S_2{}^{0C}$
SPHEROIDAL
$_0S_0{}^{0C}$
A
TORIDAL
1.0
0
10
20
30
η

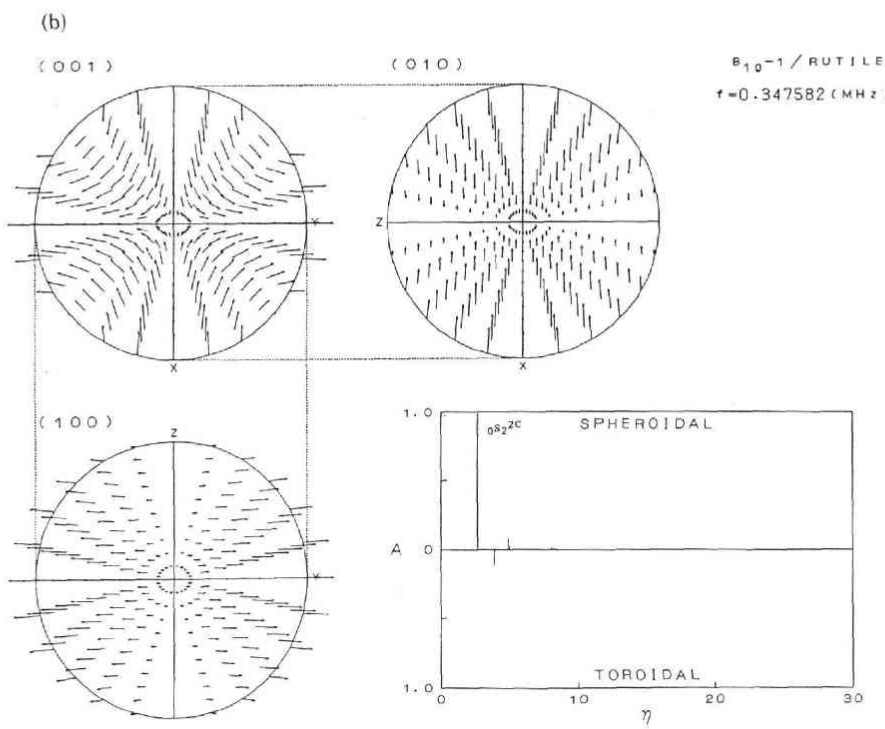
(b)
(001)
(010)
$B_{10}$-1 / RUTILE
f=0.347582 (MHz)
(100)
$_0S_2{}^{2C}$
SPHEROIDAL
A
TORIDAL
1.0
0
10
20
30
η

(c)

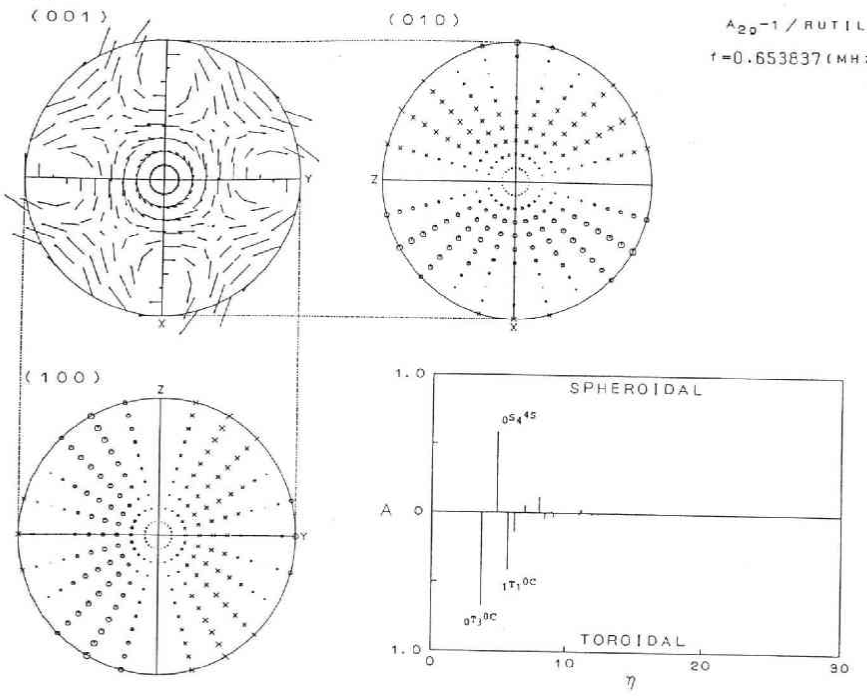
(001)
(010)
(100)
$A_{20}$-1 / RUTILE
f=0.653837(MHz)
SPHEROIDAL
TOROIDAL
A
η

(d)

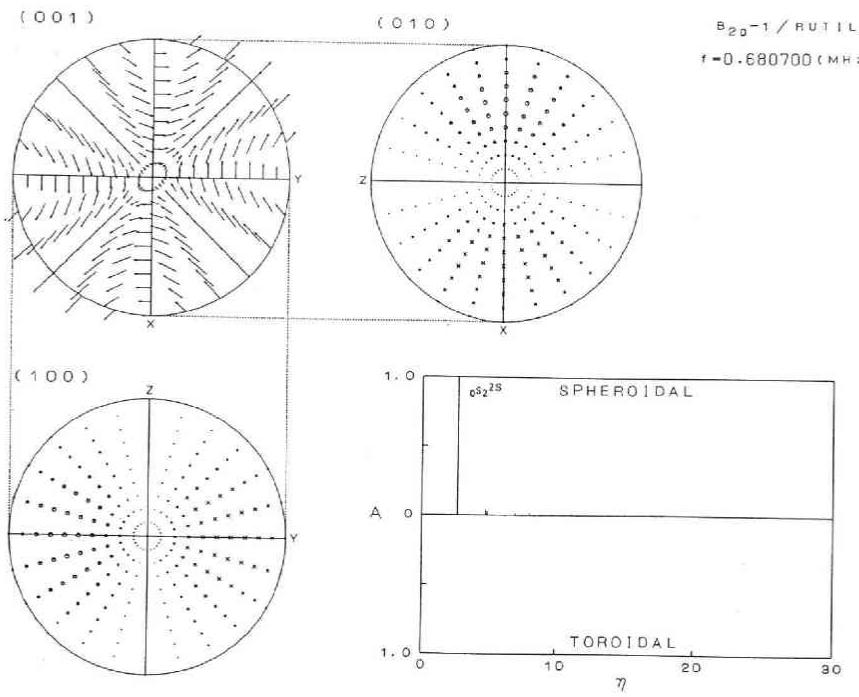
(001)
(010)
(100)
$B_{20}$-1 / RUTILE
f=0.680700(MHz)
SPHEROIDAL
TOROIDAL
A
η

(e)

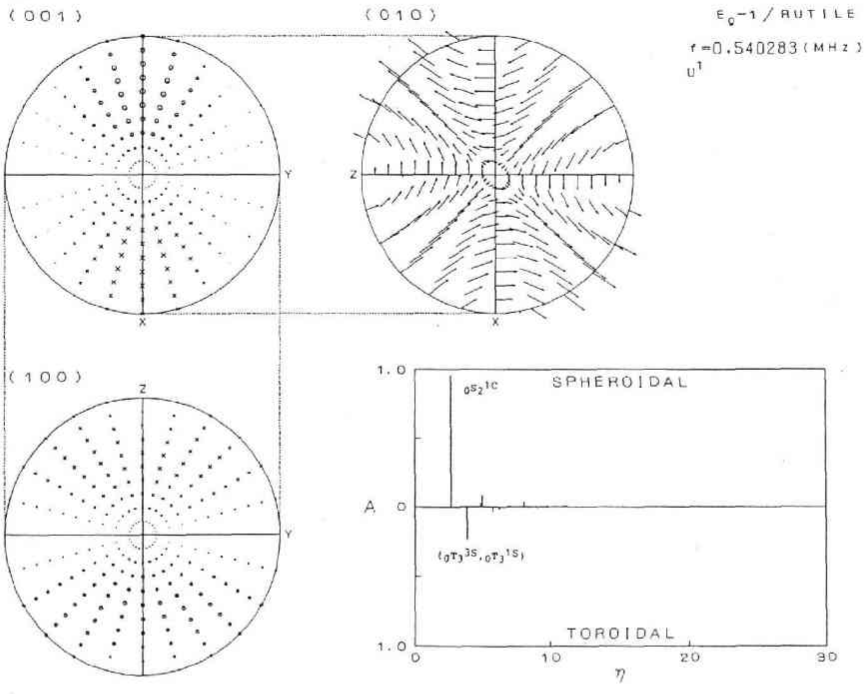
(001)
(010)
(100)
E0-1 / RUTILE
f=0.540283 (MHz)
U1
Z
Y
X
1.0
SPHEROIDAL
0S2 1C
A 0
(0T3 3S, 0T3 1S)
TOROIDAL
1.0
0
10
20
30
η

(f)

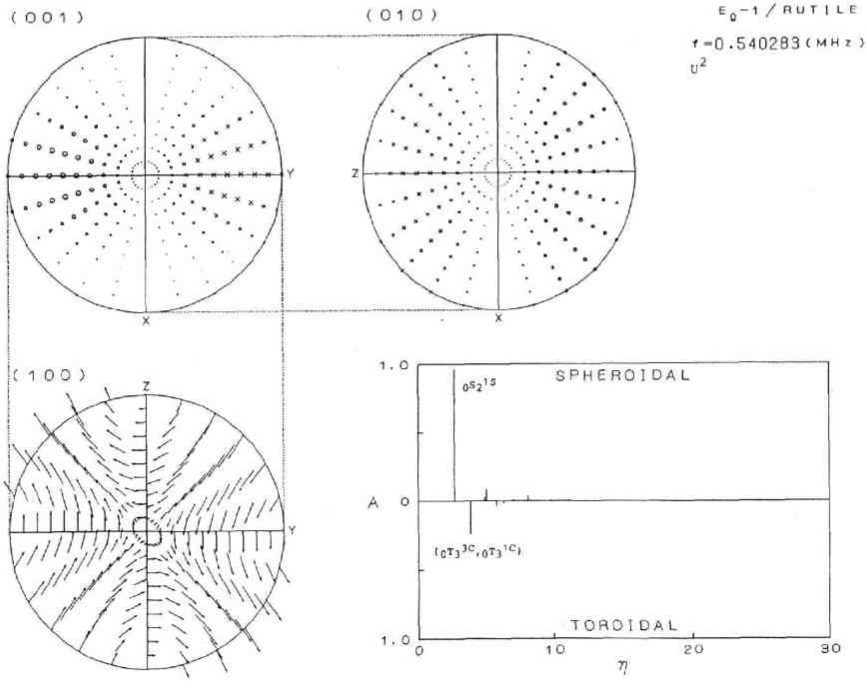
(001)
(010)
(100)
E0-1 / RUTILE
f=0.540283 (MHz)
U2
Z
Y
X
1.0
SPHEROIDAL
0S2 1S
A 0
(0T3 3C, 0T3 1C)
TOROIDAL
1.0
0
10
20
30
η

(g)

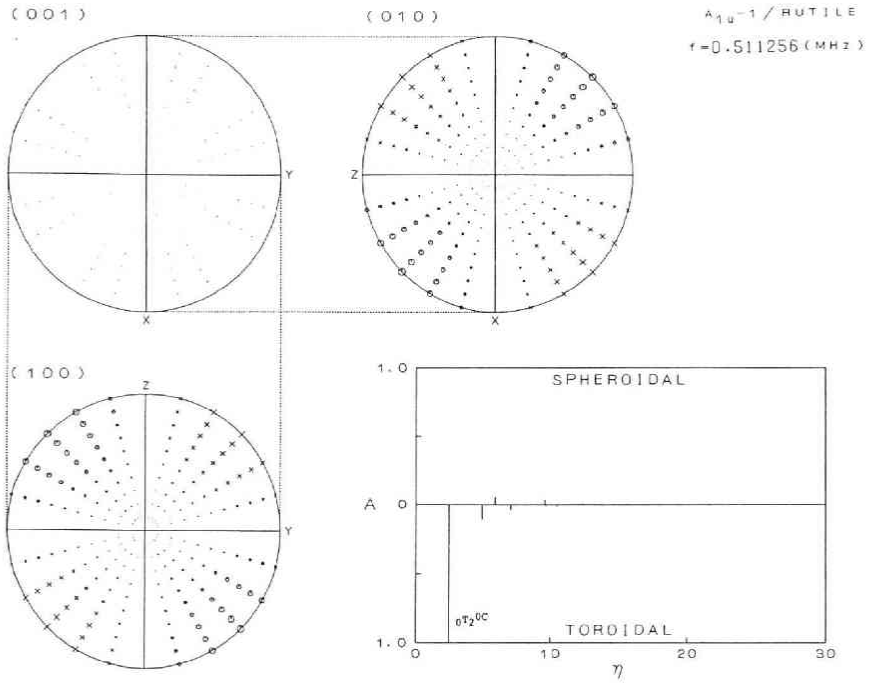
( 0 0 1 )
( 0 1 0 )
$A_{1u}$-1 / RUTILE
f=0.511256 (MHz)
Y
Z
X
( 1 0 0 )
SPHEROIDAL
A
0
$_0T_2^{0C}$
TOROIDAL
1.0
1.0
0
10
20
30
η

(h)

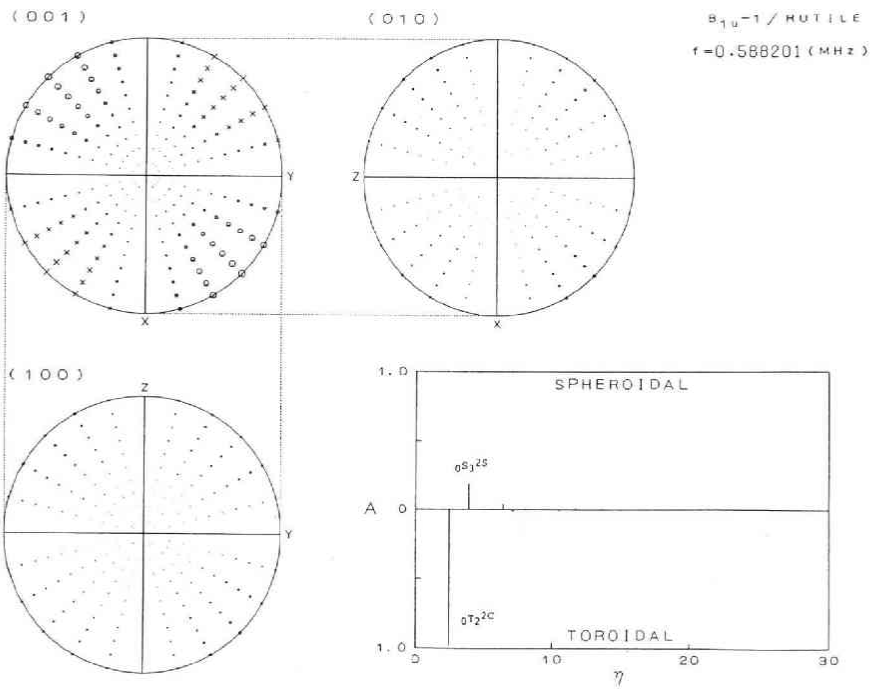
( 0 0 1 )
( 0 1 0 )
$B_{1u}$-1 / RUTILE
f=0.588201 (MHz)
Y
Z
X
( 1 0 0 )
SPHEROIDAL
$_0S_1^{2S}$
A
0
$_0T_2^{2C}$
TOROIDAL
1.0
1.0
0
10
20
30
η

(i)

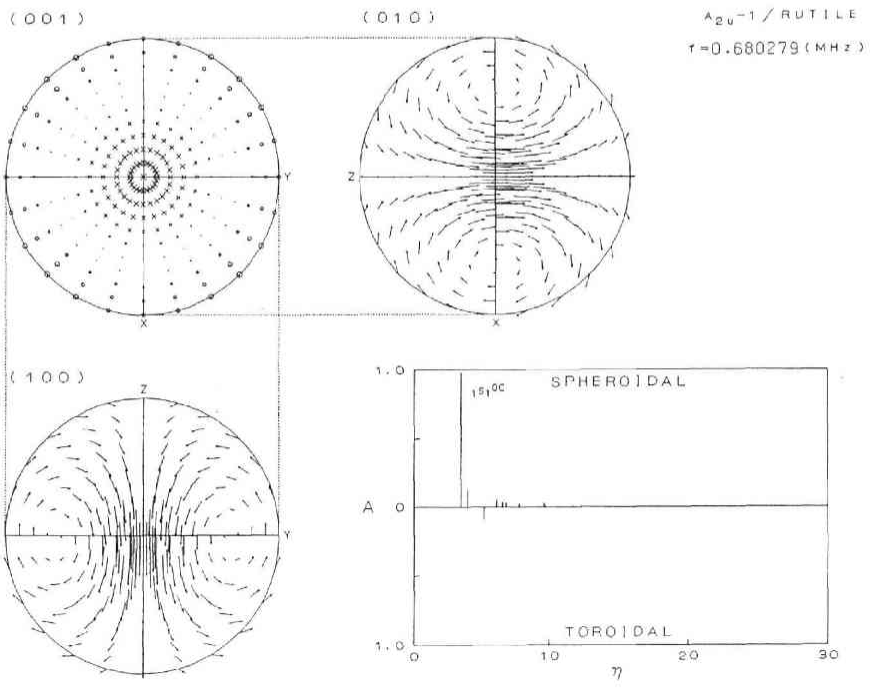
( 0 0 1 )
( 0 1 0 )
$A_{2u}$-1 / RUTILE
f=0.680279 ( MHz )
( 1 0 0 )
SPHEROIDAL
$_{1S_1}{}^{0C}$
TOROIDAL
A
1.0
0
10
20
30
η

(j)

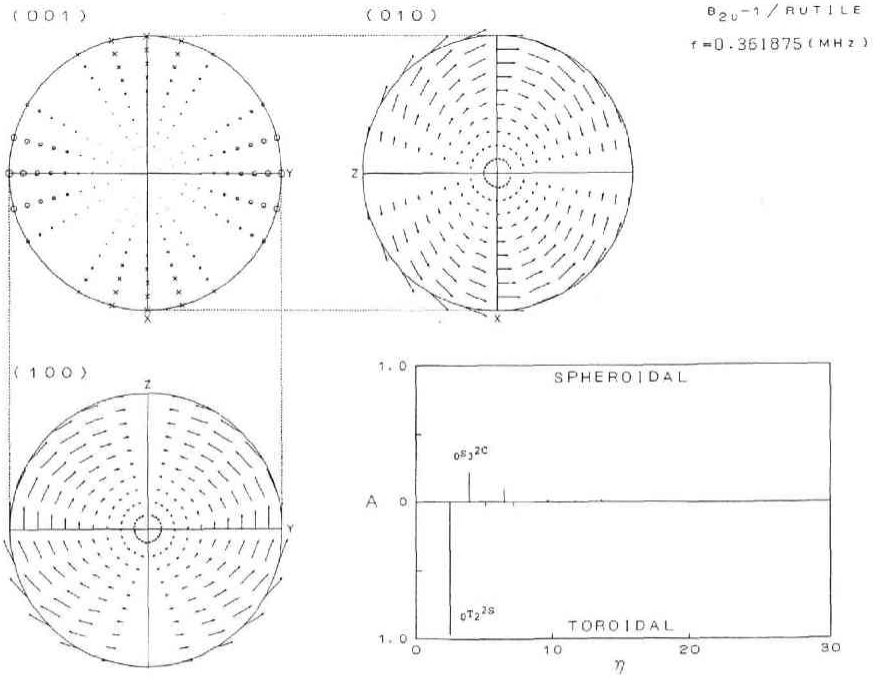
( 0 0 1 )
( 0 1 0 )
$B_{2u}$-1 / RUTILE
f=0.351875 ( MHz )
( 1 0 0 )
SPHEROIDAL
$_{0S_3}{}^{2C}$
$_{0T_2}{}^{2S}$
TOROIDAL
A
1.0
0
10
20
30
η

(k)

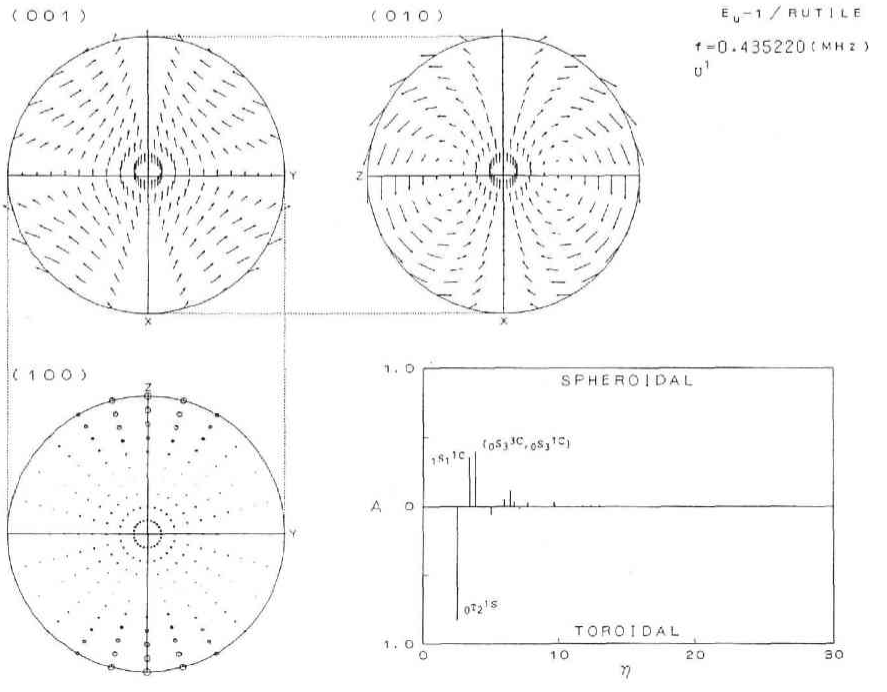
( 0 0 1 )
( 0 1 0 )
( 1 0 0 )
E$_u$-1 / RUTILE
f=0.435220 ( MHz )
$U^1$
SPHEROIDAL
TOROIDAL
A
$\eta$
1.0
0
10
20
30
$^1S_1{}^1C$
$(_0S_3{}^3C, {}_0S_3{}^1C)$
$_0T_2{}^1S$

(l)

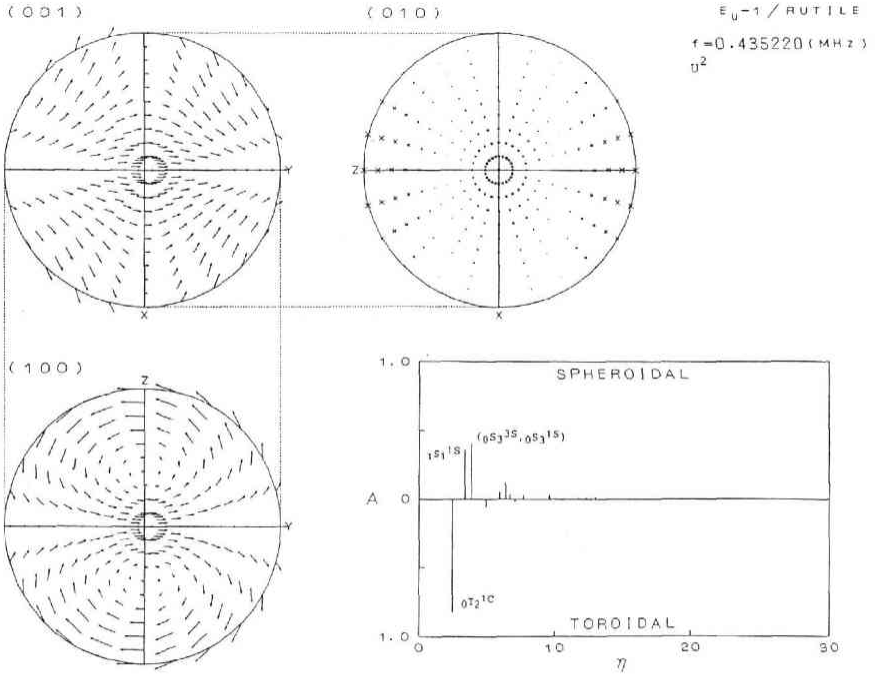
( 0 0 1 )
( 0 1 0 )
( 1 0 0 )
E$_u$-1 / RUTILE
f=0.435220 ( MHz )
$U^2$
SPHEROIDAL
TOROIDAL
A
$\eta$
1.0
0
10
20
30
$^1S_1{}^1S$
$(_0S_3{}^3S, {}_0S_3{}^1S)$
$_0T_2{}^1C$

The degree of the contribution of each basis function may be measured by the magnitude of the expansion coefficient $a_p$. However, it is not easy to compare individual $a_p$'s each other, since, in general, they are in a very large number. Here, we introduce a quantity $A(\eta)$ defined by

$$A(\eta)=\sqrt{\sum_m a_p a_p^*} \tag{11}$$

where the summation is made for the possible $m$'s having the common dimensionless eigenvalue $\eta$ specified by the orders $n$ and $l$. The $A(\eta)$ of an anisotropic mode denotes a measure of the overall contribution from the isotropic modes having various isotropic eigenvalues (*cf.*, Tsuboi *et al.*, 1985). The $A(\eta)$ for each anisotropic mode is plotted against the $\eta$ separately for spheroidal and toroidal modes in the $\eta$-$A$ diagram of Fig. 2. The eigenfunction names ${}_nO_l^{mh}$ tagged to major spectral lines in Fig. 2 show the most effective component to them, which reaches ninety percent or more in most of the fundamental modes. In the $A_{1g}-1$ mode (Fig. 2-a), for example, the ${}_0S_2{}^{0c}$ eigenfunction most effectively contributes to the mode and secondly the ${}_0S_0^{0c}$. The toroidal eigenfunctions have almost no influence on this vibration mode. This means that the displacement distribution of the $A_{1g}-1$ mode should be roughly similar to that of ${}_0S_2$ mode of the isotropic sphere, and will be discussed more later. On the other hand, the coupling between spheroidal and toroidal eigenfunctions is clearly found in the $A_{2g}-1$ mode (Fig. 2-c). The displacement distribution of the $A_{2g}-1$ is graphically shown in Fig. 3 as given by a superposition of isotropic eigenfunctions with weighting function $a_p$. The displacement pattern in the equatorial plane differs significantly from any of the isotropic patterns. Extensive couplings among isotropic eigenfunctions are also found in other fundamental modes, especially in the $E_u-1$ mode (Figs. 2-k and l).

The oscillation displacement of the $A_{1g}-1$ mode is composed mainly of the ${}_0S_2^{0c}$ eigenfunction, as already seen in Fig. 2-a. In order to show how complicated the

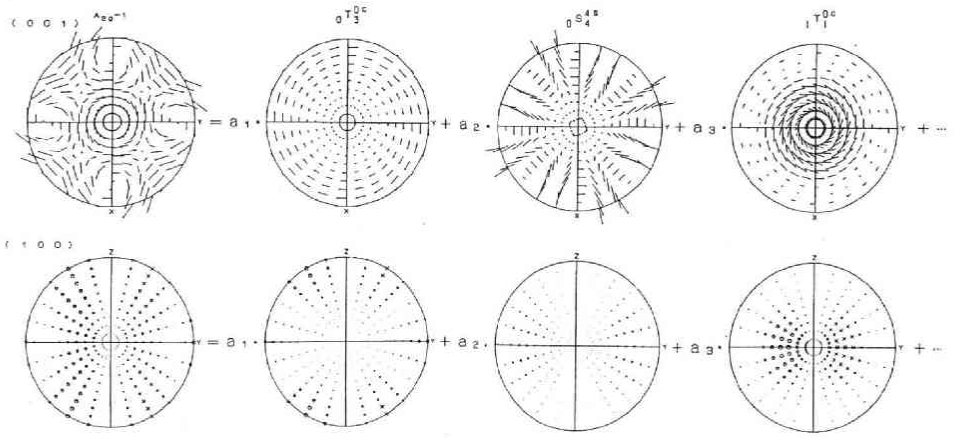

Fig. 3 Composition of displacament distribution of the $A_{2g}-1$ mode on the (001) and (100) planes. The anisotropic displacements are represented by superposition of isotropic eigenfunctions multiplied by the expansion coefficients $a_p$. See Fig. 2 for the symbols.

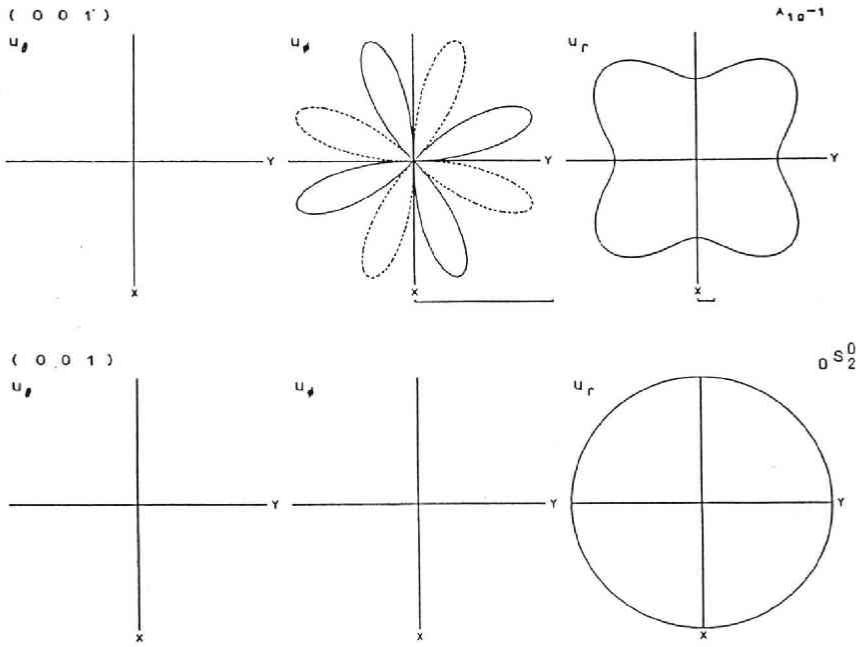


Fig. 4 Comparison of vibration displacements on the equatorial plane ($\theta=\pi/2$) between rutile and isotropic spheres with a unit radius. The top row is the polar-coordinate representation of displacement components $U_\theta$, $U_\phi$ and $U_r$ of the $A_{1g}-1$ mode of the rutile sphere and the bottom row shows those of the ${}_0S_2{}^0$ mode of the isotropic sphere, respectively. The scale bars compare the unit magnitude of the displacement components. The solid and dotted lines denote opposite signs of the vector components to each other.

vibration of the anisotropic sphere is, we compare in details the displacements of this rather simple anisotropic mode of $A_{1g}-1$ with that of the isotropic ${}_0S_2^{0c}$ mode in Fig. 4. The surface displacement vector of the ${}_0S_2^{0c}$ mode on the equatorial plane has only the radial component $U_r$ independent of the coordinate $\phi$. On the other hand, the $A_{1g}-1$ mode has both the dominant $U_r$ component and the minor $U_\phi$, as understood from the scale bars showing a unit amplitude. The component $U_r$ of $A_{1g}-1$ looks like what the $U_r$ of ${}_0S_2^{0c}$ is slightly modified to have a four-fold rotation symmetry around the $z$-axis owing to minor contribution from eigenfunctions other than ${}_0S_2^{0c}$. The components of $U_r$ and $U_\phi$ are dependent on the coordinate $\phi$ and also show the four-fold symmetry. This symmetric property of the displacement pattern results from the elastic symmetry of the point group $D_{4h}$ and is found commonly in the $A_{1g}$, $A_{2g}$, $A_{1u}$ and $A_{2u}$ modes. It is also interesting that either of $\boldsymbol{U}^1$ or $\boldsymbol{U}^2$ displacement vector of the $E_u-1$ mode, has no four-fold rotation symmetry in the equatorial plane but mirror symmetry with respect to the $x$-$y$ plane. Both the displacement patterns satisfy the symmetric constraints specified in the point group $D_{4h}$. The detailed discussion on the symmetry is made in the following section.

As seen in Figs. 2-a to 2-l, most of the fundamental modes of the rutile sphere are

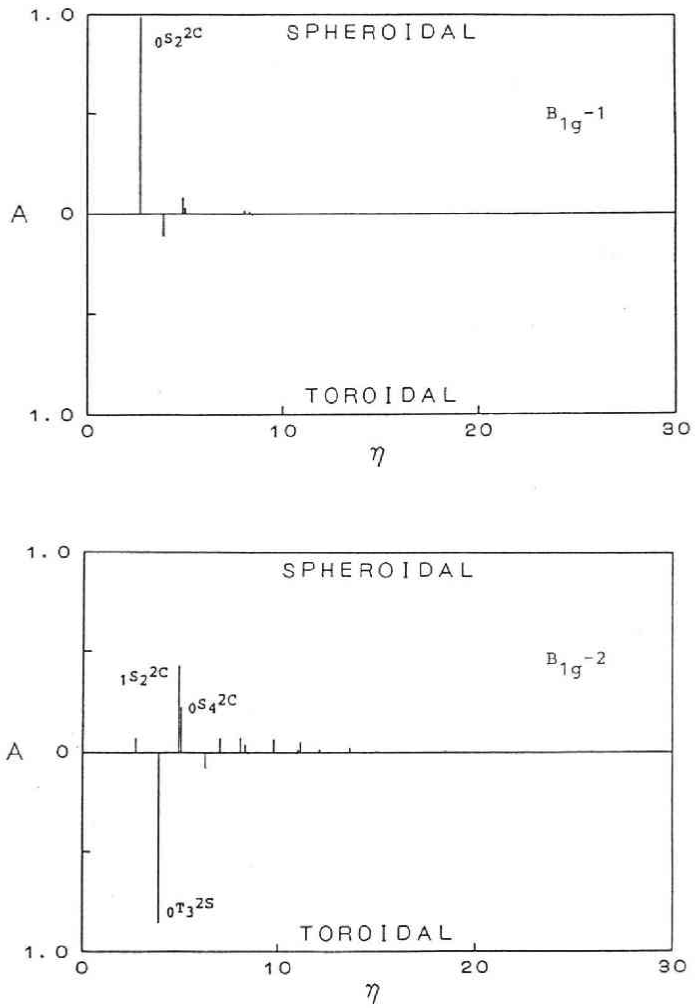


Fig. 5 Comparison of the $\eta-A$ diagram of the fundamental mode $B_{1g}-1$ with that of the first higher modes $B_{1g}-2$.

greatly governed by a single isotropic eigenfunction, and extensive coupling of spheroidal and toroidal modes is found only in the $A_{2g}-1$ and $E_u-1$ modes. Figure 5 shows the $\eta$-$A$ diagrams for the fundamental and the first higher mode of the $B_{1g}$ group. The coupling becomes more complicated in the higher mode, and this can also be found in other higher modes. This suggests that higher mode oscillations are more remarkably influenced by the anisotropic elasticity because of their shorter wavelength. Since such coupling does not take place in the free oscillation of a homogeneous isotropic sphere, this is one of the effects of anisotropic elasticity.

Table 4. Characters of the Point Group $D_{4h}$

| | $E$ | $2C_4$ | $C_4^2$ | $2C_2'$ | $2C_2''$ | $I$ | $2IC_4$ | $\sigma_h$ | $2\sigma_v$ | $2\sigma_d$ |
|---|---|---|---|---|---|---|---|---|---|---|
| $A_{1g}$ | 1 | 1 | 1 | 1 | 1 | 1 | 1 | 1 | 1 | 1 |
| $A_{2g}$ | 1 | 1 | 1 | −1 | −1 | 1 | 1 | 1 | −1 | −1 |
| $B_{1g}$ | 1 | −1 | 1 | 1 | −1 | 1 | −1 | 1 | 1 | −1 |
| $B_{2g}$ | 1 | −1 | 1 | −1 | 1 | 1 | −1 | 1 | −1 | 1 |
| $E_g$ | 2 | 0 | −2 | 0 | 0 | 2 | 0 | −2 | 0 | 0 |
| $A_{1u}$ | 1 | 1 | 1 | 1 | 1 | −1 | −1 | −1 | −1 | −1 |
| $A_{2u}$ | 1 | 1 | 1 | −1 | −1 | −1 | −1 | −1 | 1 | 1 |
| $B_{1u}$ | 1 | −1 | 1 | 1 | −1 | −1 | 1 | −1 | −1 | 1 |
| $B_{2u}$ | 1 | −1 | 1 | −1 | 1 | −1 | 1 | −1 | 1 | −1 |
| $E_u$ | 2 | 0 | −2 | 0 | 0 | −2 | 0 | 2 | 0 | 0 |

Symmetry operators have the following meaning; $E$: Identity, $C_n^m$: Counterclockwise rotation for positive integers $m$ and $n$ by $2\pi m/n$ around the $z$-axis and written $C_n$ for $m=1$, $C_n'$: Rotation by $2\pi/n$ around the $x$- or $y$-axis, $C_n''$: Rotation by $2\pi/n$ around the $x'$- or $y'$- axis which is defined in the middle direction between $x$- and $y$-axes, $I$: Inversion, $IC_n$: Inversion after the rotation $C_n$, $\sigma_h$: Mirror reflection by the $x$-$y$ plane, $\sigma_v$: that by the $z$-$x$ or $z$-$y$ plane, and $\sigma_d$: that by the $x'$-$z$ or $y'$-$z$ plane. (after Inui *et al.*, 1976)

## 4. Symmetric Properties of Displacement Distribution

Elastic properties of tetragonal crystal in a spherical shape are represented by symmetry of the point group $D_{4h}$, and the free oscillation modes are classified into ten groups as listed in Table 1. It is known in group theory that the displacement patterns of each group have to satisfy symmetric properties peculiar to the group (*e.g.*, Inui *et al.*, 1976). After a brief summary of the group theory, we examine the symmetry of the displacement distributions.

The point group $D_{4h}$ consists of ten symmetry operators of $E$, $C_4$, $C_4^2$, ..., $\sigma_d$, whose definitions are given in Table 4, and they are represented here by $G_i$ ($i=1, 2, \ldots, 10$). When we apply a symmetry operator $G_i$ to displacement vector $\boldsymbol{U}^\alpha$ of a d-fold degenerate mode of an irreducible representation $R$, we can write the symmetric operation as

$$G_i \boldsymbol{U}^\alpha = \sum_{\beta=1}^{d} \boldsymbol{U}^\beta D_{\alpha\beta}^R(G_i) \tag{12}$$

where the indices $\alpha$ and $\beta$ are integer from unity to $d$, and $D_{\alpha\beta}^R(G_i)$ denotes the $\alpha$-$\beta$ element of the "representation matrix". The matrix is characterized by the sum of its diagonal elements as

$$\chi^R(G_i) = \mathrm{Tr}\, D^R(G_i) \tag{13}$$

and the $\chi^R(G_i)$ is called a "character". The characters of symmetry operators are shown in Table 4 for irreducible representations of the point group $D_{4h}$.

In the case of non-degenerate modes ($d=1$), such as $A_{1g}$, $A_{2g}$, $B_{1g}$, $B_{2g}$, $A_{1u}$, $A_{2u}$, $B_{1u}$ and $B_{2u}$ modes, (12) is reduced to "one-dimensional representation" of either

$$G_i \boldsymbol{U}^1 = \boldsymbol{U}^1 ; \text{ for } \chi^R(G_i) = 1 \tag{14a}$$

or

$$G_i \boldsymbol{U}^1 = -\boldsymbol{U}^1 ; \text{ for } \chi^R(G_i) = -1 \tag{14b}$$

Equation (14a) indicates that the symmetry operator $G_i$ transforms the displacement $\boldsymbol{U}^1$ to itself, and (14b) shows antisymmetric transformation, which means that the displacement vectors $G_i \boldsymbol{U}^1$ are identical with the original vectors $\boldsymbol{U}^1$ in magnitude but opposite

Table 5. Representation Matrices of the $E_g$ and $E_u$ Modes, and Their Characters $\chi^R$

| Operator | | Matrix ($E_g$) | $\chi^R$ | Matrix ($E_u$) | $\chi^R$ |
|---|---|---|---|---|---|
| $E$ | | $\begin{bmatrix} 1 & 0 \\ 0 & 1 \end{bmatrix}$ | 2 | $\begin{bmatrix} 1 & 0 \\ 0 & 1 \end{bmatrix}$ | 2 |
| $2C_4$ | : $C_4$ | $\begin{bmatrix} 0 & -1 \\ 1 & 0 \end{bmatrix}$ | 0 | $\begin{bmatrix} 0 & 1 \\ -1 & 0 \end{bmatrix}$ | 0 |
| | : $C_4^{-1}$ | $\begin{bmatrix} 0 & 1 \\ -1 & 0 \end{bmatrix}$ | 0 | $\begin{bmatrix} 0 & -1 \\ 1 & 0 \end{bmatrix}$ | 0 |
| $C_4^2$ | | $\begin{bmatrix} -1 & 0 \\ 0 & -1 \end{bmatrix}$ | −2 | $\begin{bmatrix} -1 & 0 \\ 0 & -1 \end{bmatrix}$ | −2 |
| $2C_2'$ | : $C_2'(x)$ | $\begin{bmatrix} -1 & 0 \\ 0 & 1 \end{bmatrix}$ | 0 | $\begin{bmatrix} 1 & 0 \\ 0 & -1 \end{bmatrix}$ | 0 |
| | : $C_2'(y)$ | $\begin{bmatrix} 1 & 0 \\ 0 & -1 \end{bmatrix}$ | 0 | $\begin{bmatrix} -1 & 0 \\ 0 & 1 \end{bmatrix}$ | 0 |
| $2C_2''$ | : $C_2''(x')$ | $\begin{bmatrix} 0 & -1 \\ -1 & 0 \end{bmatrix}$ | 0 | $\begin{bmatrix} 0 & -1 \\ -1 & 0 \end{bmatrix}$ | 0 |
| | : $C_2''(y')$ | $\begin{bmatrix} 0 & 1 \\ 1 & 0 \end{bmatrix}$ | 0 | $\begin{bmatrix} 0 & 1 \\ 1 & 0 \end{bmatrix}$ | 0 |
| $I$ | | $\begin{bmatrix} 1 & 0 \\ 0 & 1 \end{bmatrix}$ | 2 | $\begin{bmatrix} -1 & 0 \\ 0 & -1 \end{bmatrix}$ | −2 |
| $2IC_4$ | : $IC_4$ | $\begin{bmatrix} 0 & -1 \\ 1 & 0 \end{bmatrix}$ | 0 | $\begin{bmatrix} 0 & -1 \\ 1 & 0 \end{bmatrix}$ | 0 |
| | : $IC_4^{-1}$ | $\begin{bmatrix} 0 & 1 \\ -1 & 0 \end{bmatrix}$ | 0 | $\begin{bmatrix} 0 & 1 \\ -1 & 0 \end{bmatrix}$ | 0 |
| $\sigma_h$ | | $\begin{bmatrix} -1 & 0 \\ 0 & -1 \end{bmatrix}$ | −2 | $\begin{bmatrix} 1 & 0 \\ 0 & 1 \end{bmatrix}$ | 2 |
| $2\sigma_v$ | : $\sigma(x)$ | $\begin{bmatrix} 1 & 0 \\ 0 & -1 \end{bmatrix}$ | 0 | $\begin{bmatrix} 1 & 0 \\ 0 & -1 \end{bmatrix}$ | 0 |
| | : $\sigma(y)$ | $\begin{bmatrix} -1 & 0 \\ 0 & 1 \end{bmatrix}$ | 0 | $\begin{bmatrix} -1 & 0 \\ 0 & 1 \end{bmatrix}$ | 0 |
| $2\sigma_d$ | : $\sigma(x')$ | $\begin{bmatrix} 0 & 1 \\ 1 & 0 \end{bmatrix}$ | 0 | $\begin{bmatrix} 0 & -1 \\ -1 & 0 \end{bmatrix}$ | 0 |
| | : $\sigma(y')$ | $\begin{bmatrix} 0 & -1 \\ -1 & 0 \end{bmatrix}$ | 0 | $\begin{bmatrix} 0 & 1 \\ 1 & 0 \end{bmatrix}$ | 0 |

See Table 4 for symmetry operators.

in direction. In such a manner, the character $\chi^R$ in one-dimensional case specifies the symmetric properties of the displacement pattern.

On the other hand, the $E_g$ and $E_u$ modes are two-fold degenerate ($d=2$), and (12) is written by "two-dimensional representation" as

$$G_i(\boldsymbol{U}^1, \boldsymbol{U}^2)=(\boldsymbol{U}^1, \boldsymbol{U}^2)\begin{pmatrix} D^R_{11}(G_i) & D^R_{12}(G_i) \\ D^R_{21}(G_i) & D^R_{22}(G_i) \end{pmatrix} \tag{15}$$

where $\boldsymbol{U}^1$ or $\boldsymbol{U}^2$ is either of congruent displacements of a two-fold degenerate mode. The representation matrices for the $E_g$ and $E_u$ modes are shown in Table 5 for all the symmetry operators with their characters. For example, when an operator $C_4$ is applied to displacements of the $E_u$ mode, (15) is written as

$$C_4(\boldsymbol{U}^1, \boldsymbol{U}^2)=(\boldsymbol{U}^1, \boldsymbol{U}^2)\begin{pmatrix} 0 & 1 \\ -1 & 0 \end{pmatrix} \tag{16}$$

and therefore we obtain

$$C_4\boldsymbol{U}^1=-\boldsymbol{U}^2 \tag{17a}$$

$$C_4\boldsymbol{U}^2=\boldsymbol{U}^1. \tag{17b}$$

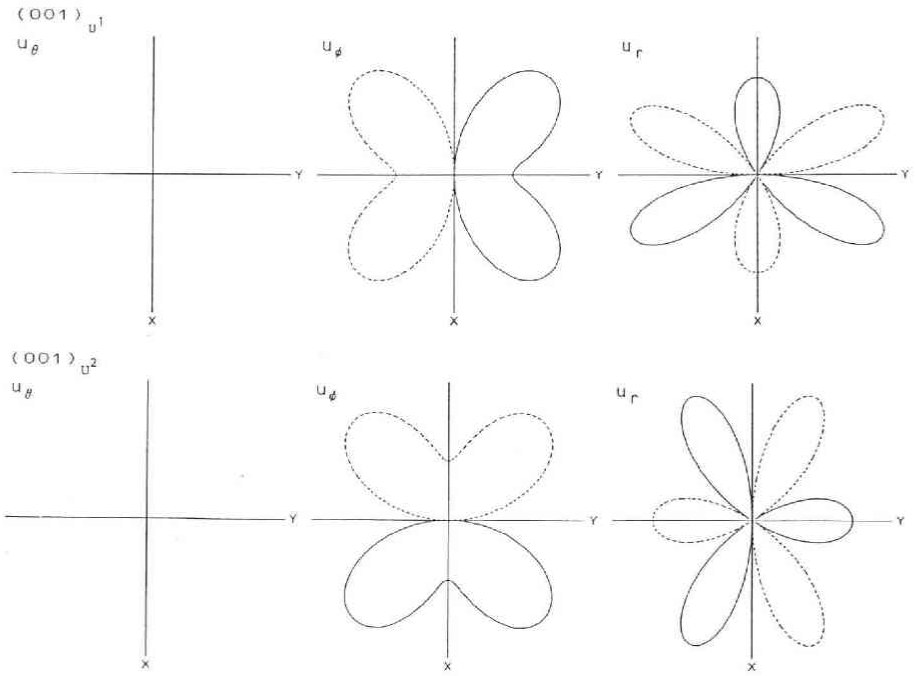


Fig. 6 The polar-coordinate representation of displacement components on the equatorial plane for $\boldsymbol{U}^1$ and $\boldsymbol{U}^2$ of the degenerate $E_u-1$ mode. See Fig. 4 for the solid and dotted lines.

These indicate that the displacement vector $\boldsymbol{U}^1$ is anti-symmetric to the $\boldsymbol{U}^2$ for the rotation $C_4$, but the $\boldsymbol{U}^2$ coincides with the $\boldsymbol{U}^1$ for the same rotation. When the computed displacement patterns satisfy (14) or (15) for all the symmetric operators, we can say that they satisfy the symmetric constraints specified by the representation matrices. This is confirmed for all the displacement patterns of oscillation modes up to several higher modes in each group.

We see here some details on the $A_{2g}-1$ and $E_u-1$ modes, as examples for one- and two-dimensional representations. Examining the displacement vectors of the $A_{2g}-1$ on the $x$-$y$ plane in Fig. 2-b, the displacement pattern is found to be symmetric ($\chi^R=1$) for the operators $E$, $C_4$, $C_4^2$ and $IC_4$ and anti-symmetric ($\chi^R=-1$) for the $C_2'$, $C_2''$, $\sigma_v$ and $\sigma_d$. The displacement on the $y-z$ plane shows that the $I$ and $\sigma_h$ are also symmetric transformation operators ($\chi^R=1$). After all, the displacement pattern of the $A_{2g}-1$ mode satisfies the symmetry properties required by the characters in Table 4.

In order to examine the symmetric properties of two-fold degenerate modes, we simply show azimuthal dependence of displacements $\boldsymbol{U}^1$ and $\boldsymbol{U}^2$ of the $E_u-1$ mode on the equatorial plane (Fig. 6). They have no $U_\theta$ component. The displacement pattern of $\boldsymbol{U}^1$ is anti-symmetric to $\boldsymbol{U}^2$ for the rotation $C_4$, while the $\boldsymbol{U}^2$ coincides with the $\boldsymbol{U}^1$ for the $C_4$. This symmetry relation between $\boldsymbol{U}^1$ and $\boldsymbol{U}^2$ is expressed by (16). Multiplying each matrix in Table 5 to ($\boldsymbol{U}^1$, $\boldsymbol{U}^2$), we find that (15) holds. The operator $\sigma_h$ can also be found to work on the displacement patterns in the other sections as a symmetric operator (see Figs. 2-k and 2-l). Therefore, both of $\boldsymbol{U}^1$ and $\boldsymbol{U}^2$ satisfy all the symmetric properties required by the representation matrices.

## 5. Conclusion

Free oscillation eigenfrequencies and displacements have been computed for a homogeneous elastic sphere with tetragonal crystal symmetry. The anisotropic sphere vibrates in much more complicated manner than an isotropic sphere, and the degree of the effect of anisotropic elasticity varies from mode to mode. From satisfactory agreement between the observed and computed eigenfrequencies and from examination of the symmetric properties of the computed displacement patterns, we conclude that the present algorithm and computer programs are correctly composed. The obtained results are summarized as follows:

1) All the computed displacement patterns satisfy the symmetric constraints required from the point group $D_{4h}$.

2) The effect of anisotropic elasticity appears to be controlled by the different degree of coupling among spheroidal and toroidal modes of the isotropic sphere used as the basis functions, and is more remarkable in higher modes of each group.

3) Each two-fold degenerate mode has two displacement patterns which are geometrically congruent, but mechanically independent.

4) Most of the modes have a pair or more of nodal points on the spherical surface. Carefulness in measurement is required in detection and identification of oscillation modes.

*Acknowledgements*: The authors acknowledge Prof. Tomowo Hirasawa for inviting this paper to this special volume and also for reading the manuscript. They are also grateful to Prof. Mineo Kumazawa for his helpful comments.

## References

Inui, T., Y. Tanabe and Y. Onodera, 1976: *Group theory and its application in physics*, Syokabo, Tokyo Japan, 1-425.

Isoda, S., 1989: Computation of free oscillation eigenfrequency of elastically anisotropic spheres: A base for the resonant sphere technique, in Japanese, *Master Thesis*, Okayama Univ., 1-143.

Jordan, T.H. and D.L. Anderson, 1974: Earth structure from free oscillation and travel times, *Geophys. J.*, **63**, 411-459.

Kumazawa, M., 1964: The elastic constants of rocks in terms of elastic constants of constituent mineral grains, petrofabric and interface structures, *J. Earth Science, Nagoya University*, **12**, 147-176.

Lamb, H., 1882: On the vibrations of an elastic sphere, *Proc. Lond. Math. Soc.*, **13**, 189-212.

Mochizuki, E., 1986: The free oscillations of an anisotropic and heterogeneous earth, *Geophys. J.*, **86**, 167-176.

Mochizuki, E., 1988: Sphere-resonance method to determine elastic constants of crystal, *J. Appl. Phys.*, **63**, 5668-5673.

Morelli, A., A.M. Dziewonski and J.H. Woodhouse, 1986: Anisotropy of the inner core inferred from PKIKP travel times, *Geophys. Res. Lett.*, **13**, 1545-1548.

Oda, H., S. Isoda, I. Suzuki and K. Seya, 1988: Free oscillation frequencies and their partial derivatives of anisotropic spheres, *Eos Trans. Am. Geophys. Union*, **69**, 1408.

Oda, H., I. Suzuki, S. Isoda, and K. Seya, 1989: An application of the resonant sphere techique to periclase, Abstract of the Symposium, *Phase transformation at high pressures and high temperatures: Applications to geophysical and petrological problems*, 20-21.

Ohno, I., 1976: Free vibration of a rectangular parallelepiped crystal and its application to determination of elastic constants of orthorhombic crystal, *J. Phys. Earth*, **24**, 355-379.

Phinney, R.A. and R. Burridge, 1973: Representation of the elastic-gravitational excitation of a spherical earth model, by generalized spherical harmonics, *Geophys. J.*, **34**, 451-487.

Sato, Y. and T. Usami, 1962: Basic study on the oscillation of a homogeneous elastic sphere (I-III), *Geophys. Mag.*, **31**, 15-62.

Soga, N. and O.L. Anderson, 1967: Elastic properties of tektites measured by resonant sphere technique, *J. Geophys. Res.*, **72**, 1733-1739.

Suetsugu, D. and I. Nakanishi, 1987: Regional and azimuthal dependence of phase velocities of mantle Rayleigh waves in the Pacific Ocean, *Phys. Earth Planet. Interiors*, **47**, 230-245.

Suzuki, I., S. Isoda, H. Oda, T. Saito and K. Seya, 1988: Determination of elastic constants of a crystal by means of the resonant sphere technique: An application to rutile, *Eos Trans. Am. Geophys. Union*, **69**, 1408.

Tsuboi, S., R.J. Geller and S.P. Morris, 1985: Partial derivatives of the eigenfrequency of a laterally heterogeneous earth, *Geophys. Res. Lett.*, **12**, 817-820.

Wachtman, J.B.Jr., W.E. Tefft and D.G. Lam Jr., 1962: Elastic constants of rutile ($TiO_2$), *J. Res. Nat. Bur. Stand.*, **66A**, 465-471.

Woodhouse, J.H., D. Giardini and X-.D. Li, 1986: Evidence of inner core anisotropy from free oscillations, *Geophys. Res. Lett.*, **13**, 1549-1552.